A new F-18-labeled fluoroacetylmorpholino derivative of vesamicol for neuroimaging of the vesicular acetylcholine transporter

12 AUTHORS, INCLUDING:

Steffen Fischer
Helmholtz-Zentrum Dresden-Rossendorf
77 PUBLICATIONS **469** CITATIONS

SEE PROFILE

Johnny Vercouillie
University of Tours
59 PUBLICATIONS **564** CITATIONS

SEE PROFILE

Achim Hiller
Helmholtz-Zentrum Dresden-Rossendorf
48 PUBLICATIONS **526** CITATIONS

SEE PROFILE

Peter Brust
Helmholtz-Zentrum Dresden-Rossendorf
203 PUBLICATIONS **2,076** CITATIONS

SEE PROFILE

A new ^{18}F-labeled fluoroacetylmorpholino derivative of vesamicol for neuroimaging of the vesicular acetylcholine transporter[☆]

Dietlind Sorger[a,*], Matthias Scheunemann[b], Udo Großmann[a], Steffen Fischer[b], Johnny Vercouille[b], Achim Hiller[b], Barbara Wenzel[b], Ali Roghani[c], Reinhard Schliebs[d], Peter Brust[b], Osama Sabri[a], Jörg Steinbach[b]

[a]Department of Nuclear Medicine, University of Leipzig, 04103 Leipzig, Germany
[b]Institute of Interdisciplinary Isotope Research, 04318 Leipzig, Germany
[c]Department of Pharmacology and Neuroscience, Texas Tech University Health Sciences Center, Lubbock, TX 39430, USA
[d]Paul-Flechsig Institute of Brain Research, University of Leipzig, 04109 Leipzig, Germany

Abstract

With the aim of producing selective radiotracers for in vivo imaging of the vesicular acetylcholine transporter (VAChT) using positron mission tomography (PET), here, we report synthesis and analysis of a new class of conformationally constrained vesamicol analogues with moderate lipophilicity. The sequential ring opening on *trans*-1,4-cyclohexadiene dioxide enabled an approach to synthesize 6-arylpiperidino-octahydrobenzo[1,4]oxazine-7-ols [morpholino vesamicols]. The radiosynthesis of the [^{18}F]fluoroacetyl-substituted derivative ([^{18}F]FAMV) was achieved starting from a corresponding bromo precursor [2-Bromo-1-[7-hydroxy-6-(4-phenyl-piperidin-1-yl)-octahydro-benzo[1,4] oxazin-4-yl]-ethanone] and using a modified commercial computer-controlled module system with a radiochemical yield of 27±4%, a high radiochemical purity (99%) and a specific activity of 35 GBq/μmol. In competitive binding assays using a PC12 cell line overexpressing VAChT and [^{3}H]-(−) vesamicol, 2-fluoro-1-[7-hydroxy-6-(4-phenyl-piperidin-1-yl)-octahydro-benzo[1,4]oxazin-4-yl]-ethanone (FAMV) demonstrated a high selectivity for binding to VAChT (K_i: 39.9±5.9 nM) when compared to its binding to sigma$_{1/2}$ receptors (K_i>1500 nM). The compound showed a moderate lipophilicity (logD$_{(pH\ 7)}$=1.9) and a plasma protein binding of 49%. The brain uptake of [^{18}F]FAMV was about 0.1% injected dose per gram at 5 min after injection and decreased continuously with time. Notably, an increasing accumulation of radioactivity in the lateral brain ventricles was observed. After 1 h, the accumulation of [^{18}F]FAMV, expressed as ratio to the cerebellum, was 4.5 for the striatum, 2.0 for the cortical and 1.5 for the hippocampal regions, measured on brain slices using ex vivo autoradiography. At the present time, 75% of [^{18}F]FAMV in the plasma was shown to be metabolized to various hydrophilic compounds, as detected by high-performance liquid chromatography. The degradation of [^{18}F]FAMV was also detected in brain extracts as early as 15 min post injection (p.i.) and increased to 50% at 1 h postinjection. In conclusion, although the chemical properties of [^{18}F]FAMV and the selectivity of binding to VAChT appear to be promising indicators of a useful PET tracer for imaging VAChT, a low brain extraction, in combination with only moderate specific accumulation in cholinergic brain regions and an insufficient in vivo stability prevents the application of this compound for neuroimaging in humans.

1. Introduction

The role of the cholinergic system in Alzheimer's disease (AD) has become increasingly important, since there has been a recognition of interrelationships between an impaired cortical cholinergic function and other pathological features of the disease, such as β-amyloid formation/deposition and local inflammatory up-regulation [1,2]. Early studies on postmortem brains of patients with AD had shown that a loss of cholinergic neurons in the basal forebrain [3] was associated with a decreased activity of choline acetyltransferase (ChAT), the biosynthetic enzyme for acetylcholine, in that region and also in cortical target areas [4–6]. The gene

encoding ChAT is closely linked with the gene for the vesicular acetylcholine transporter (VAChT), where the entire VAChT coding region is localized within the first intron of the ChAT gene. This unique genetic organization is commonly referred to as the "cholinergic gene locus" [7–9]. This unique feature permits coordinated expression of the two genes throughout the adult nervous system and during development [7,10]. Hence, there is evidence from auto-radiographic studies that the VAChT density is decreased in patients with AD [11]. Studies in rats treated with β-amyloid peptide indicate that an observed reduction in VAChT density is related to the memory impairment assumed to be induced by β-amyloid [12]. These studies were performed with ^3H-labeled phenylpiperidinyl cyclohexanol (vesami-col), which binds with high affinity to an allosteric binding site on the VAChT protein [13–16], thus providing the potential possibility to use this compound and its other radiolabeled derivatives for measuring cholinergic neuronal changes in vitro and in vivo.

In rats, [^3H]vesamicol [17], [^{125}I]iodobenzovesamicol (IBVM) [18] and [^{123}I]IBVM [19], were used for autoradio-graphic studies which indicated a cholinergic synaptic loss in the cortex and the hippocampus caused by a specific cholinergic lesion in the basal forebrain. In studies on postmortem human brain tissue of patients with AD, a dissociation between ChAT activity and [^3H]vesamicol binding to VAChT was observed [11,20,21]. When the more specific radioligand (+) [^{125}I]iodobenzyltrozamicol was used, a correlation of $r=.72$ between both cholinergic parameters was found [22]. The first and so far the only application for human in vivo VAChT brain imaging has been reported using 5-[^{123}I]iodobenzovesamicol [23]. Moreover, in patients with AD and Parkinson's disease a decreased cortical binding of this radioligand was reported [24].

Despite these efforts radiochemists are still confronted with the clinical demand to develop a PET radioligand appropriate to image the presynaptic cholinergic function-ality in vivo [25]. Detailed in vitro analyses performed for a large number of vesamicol derivatives revealed their high affinity binding to VAChT but a lack of selectivity. More importantly, the binding to sigma receptors, which are widely distributed in the brain, seems to represent the main problem to be solved when new radioligands for VAChT binding are developed [26,27]. Because of the unique vesamicol binding site on VAChT, efforts are underway to synthesize new derivatives based on the vesamicol structure [28–34].

It was the intention of this study to develop a structurally modified vesamicol analogue which can be easily labeled with ^{18}F and presents a high selectivity in binding to VAChT. We aimed at a compound of moderate lipophilicity distinguished by a sufficient penetration of the blood–brain barrier and a specific accumulation in brain regions of high cholinergic densities. Based on these requirements, a novel class of conformationally fixed vesamicol analogues was synthesized by a sequential ring opening approach, starting
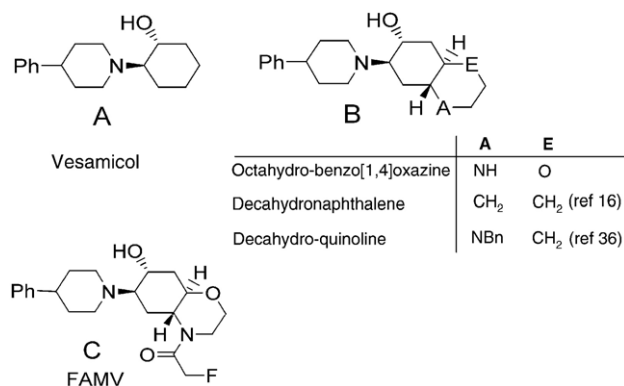

Fig. 1. Structures of vesamicol (A) and its two derivatives (B and C) used for radiotracer development for neuroimaging of VAChT.

from *trans*-1,4-cyclohexadiene dioxide [35]. The synthe-sized 6-amino-octahydrobenzo[1,4]oxazine-7-ol scaffold closely resembles to the decahydronaphthalene and decahy-droquinoline substructure, both of which have been used recently as constituents of highly potent VAChT ligands (Fig. 1B) [16,36].

Here, we report on a fluoroacetyl-octahydro[1,4]benzox-azine derivative of vesamicol [2-fluoro-1-[7-hydroxy-6-(4-phenyl-piperidin-1-yl)-octahydro-benzo[1,4]oxazin-4-yl]-ethanone (FAMV)] (Fig. 1C) including (i) the radiosynthesis of its ^{18}F-labeled derivative, (ii) its binding affinity and specificity to VAChT in vitro, (iii) its in vivo distribution and rat brain uptake as well as (iv) its metabolism in the blood and the brain.

2. Materials and methods

2.1. Chemistry

A method to synthesize the parent secondary amine (Fig. 2, compound **5**) was described in detail elsewhere [35]. Briefly, it involves a sequential ring opening of di-epoxide (**1**) with 4-phenylpiperidine (**2**) to obtain the monoepoxide (**3**) which was converted via a six-step sequence to racemic octahydro-6-(4-phenylpiperidin-1-yl)-2*H*-benzo[b][1,4]oxazin-7-ol (**5**). Both acyl derivatives [FAMV and 2-Bromo-1-[7-hydroxy-6-(4-phenyl-piperidin-1-yl)-octahydro-benzo[1,4]oxazin-4-yl]-ethanone (BrAMV)] were obtained from **5**, and the corresponding acyl halide was synthesized by applying a standard acylation procedure.

2.1.1. 2-Fluoro-1-[7-hydroxy-6-(4-phenyl-piperidin-1-yl)-octahydro-benzo[1,4]oxazin-4-yl]-ethanone

A two-phase-system consisting of a solution of the amine **5** (160 mg, 505 μmol) in CH_2Cl_2 (4 ml) and a mixture of $NaHCO_3$ (0.42 g, 5.0 mmol) in H_2O (3 ml) was stirred at 0–2°C. A solution of fluoroacetylchloride (37 μl, 50 mg, 518 μmol) in CH_2Cl_2 (1.0 ml) was added within 20 min. The cooling bath was removed, and after being stirred for 3 h, the organic layer was separated and the aqueous layer was extracted with CH_2Cl_2 (2×3 ml). The combined organic
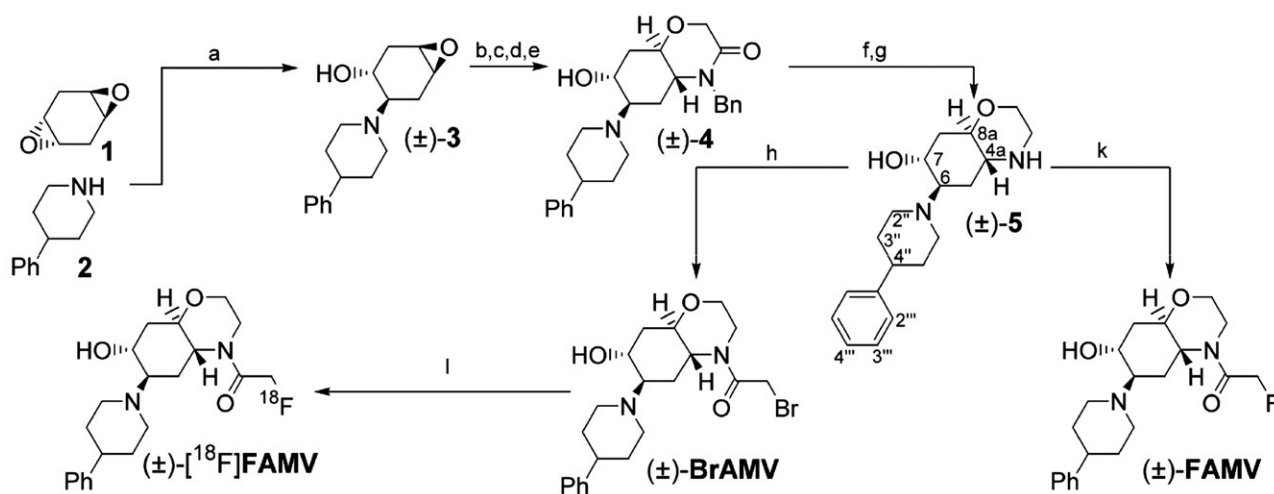
Fig. 2. Synthetic and radiosynthetic route to the VAChT binding ligand [^{18}F]FAMV; reagents and conditions [35] (b) NH$_3$.(30% aqueous solution), EtOH, 85–90°C, 10 h [99%] (c) i. PhCHO, MeOH, 0°C, 5h; ii. NaBH$_4$, −5°C, 1 h [86%, two steps] (d) ClCH$_2$COCl, NaHCO$_3$, H$_2$O, CH$_2$Cl$_2$ [94%]; (e) i-PrONa, i-PrOH, 0–2°C [96%]; (f) BH$_3$·S(CH$_3$)$_2$, THF; reflux, 1 h [99%]; (g) Pd-C, H$_2$, EtOH, 22°C [91%]; (h) BrCH$_2$COBr, NaHCO$_3$, CH$_2$Cl$_2$, 0–3°C [84%]; (k) FCH$_2$COBr, NaHCO$_3$, CH$_2$Cl$_2$, 0–3°C [84%]; (l) [^{18}F]K(Kryptofix2.2.2.)F, DMF, 145–155°C, 15 min, [RCY: 30%].

phases were dried (Na$_2$SO$_4$), filtered and evaporated to leave a solid residue (211 mg), which was recrystallized from ethyl acetate (1.5 ml) to yield FAMV [160 mg (84%)]. TLC: R$_f$=0.54 [CHCl$_3$, MeOH, aq. NH$_3$ (30%); 5:1:0.15]. Colorless crystals, Mp=178–179°C. ^{1}H NMR (400.02 MHz, CDCl$_3$): δ 1.64–1.88 (m, 4H, piperidine: 3″-H$_2$, 5″-H$_2$), 1.87–2.13 (m, 6H, 5-H$_a$, 8-H$_2$, OH, piperidine: 2″-H$_a$, 6″-H$_a$), 2.36 (m, 1H, 6-H), 2.51 (tt, J=12.1, 3.9 Hz, 1H, piperidine: 4″-H), 2.74 (m, 1H, 5-H$_b$), 3.09 (m, 1H, piperidine: 2″-H$_b$ [or 6″-H$_b$]), 3.43 (ddd, J=14.1, 4.7, 4.7 Hz, 1H, 3-H$_a$), 3.57 (m, 1H, piperidine: 6″-H$_b$ [or 2″-H$_b$]), 3.71 (ddd, J=14.1, 7.8, 3.9 Hz, 1H, 3-H$_b$), 3.84 (m, 1H, 4a-H), 3.90 (m, 1H, 2-H$_a$), 3.97 (m, 1H, 2-H$_b$), 4.04 (m, 1H, 8a-H), 4.28 (m, 1H, 7-H [CH–OH]), 4.87, 4.98 (2s [rotamers], 2H, CH$_2$F),7.16–7.24 (m, 3H$_{ar}$, 4‴-H, 2‴-H, 6‴-H), 7.27–7.32 (m, 2H$_{ar}$, 3‴-H, 5‴-H). ^{13}C NMR/^{13}C NMR-APT (100.58 MHz, CDCl$_3$): δ$_C$ 24.34 (1C$_{sec}$, 5-C), 33.73 (1C$_{sec}$, 8-C), 34.10 (1C$_{sec}$, 3″-C [or 5″-C]), 34.14 (1C$_{sec}$, 5″-C [or 3″-C]), 41.94 (d, $^4J_{CF}$=4.4 Hz, 1C$_{sec}$, 3-C), 42.86 (1C$_{tert}$, 4″-C), 50.14 (1C$_{sec}$, 6″-C [or 2″-C]), 52.66 (1C$_{sec}$, 2″-C [or 6″-C]), 57.02 (d [not resolved], 1C$_{tert}$, 4a-C), 64.76 (1C$_{tert}$, 6-C), 66.32 (1C$_{sec}$, 2-C), 66.70 (1C$_{tert}$, 7-C), 71.05 (1C$_{tert}$, 8a-C), 80.46 (d, $^1J_{CF}$=181.3 Hz, 1C$_{sec}$, FCH$_2$C=O), 126.19 (1C$_{tert}$, 4‴-C), 126.94 (2C$_{tert}$, 2‴-C, 6‴-C), 128.49 (2C$_{tert}$, 3‴-C, 5‴-C), 146.52 (1C$_{qu}$, 1‴-C), 167.54 (d, $^2J_{CF}$=17.7 Hz, 1C$_{qu}$, FCH$_2$C=O). ^{19}F NMR (CDCl$_3$, 376.39 MHz) δ$_F$ -223.32 (t, J=47.0 Hz, 1F). MS (ESI) m/z 377.22 {(M+H)$^+$, 100%}. Anal. (C$_{21}$H$_{29}$FN$_2$O$_3$) Calculated C: 67.00, H: 7.76, N: 7.44; found C: 66.77, H: 8.02, N: 7.49.

2.1.2. 2-Bromo-1-[7-hydroxy-6-(4-phenyl-piperidin-1-yl)-octahydro-benzo[1,4]oxazin-4-yl]-ethanone

The amine 5 (95 mg, 300 μmol) and bromoacetylbromide (29 μl, 65 mg, 320 μmol) were reacted in a two-phase system at 0–2°C, and the reaction mixture was worked up according to the protocol described for the preparation of the fluoroderivative. The solvent was evaporated to leave a viscous residue (147 mg), which was triturated with ethyl acetate (0.8 ml) to yield BrAMV [110 mg (84%)]. TLC: R$_f$=0.25 [CHCl$_3$, MeOH, aq. NH$_3$ (30%); 10:1:0.1]. Colorless crystals, Mp=175–182°C (decomposition). ^{1}H NMR (300.05 MHz, CDCl$_3$): δ 1.64–2.16 (several m, 10H, 5-H$_a$, 8-H$_2$, OH, piperidine: 3″-H$_2$, 5″-H$_2$, 2″-H$_a$, 6″-H$_a$), 2.38 (m, 1H, 6-H), 2.51 (tt, J=12.0, 4.1 Hz, 1H, piperidine: 4″-H), 2.64 (m, 1H, 5-H$_b$), 3.09 (m, 1H, piperidine: 2″-H$_b$ [or 6″-H$_b$]), 3.51-3.62 (m, 2H, 3-H$_a$, piperidine: 6″-H$_b$ [or 2″-H$_b$]), 3.82 (ddd, J=13.5, 9.4, 4.1 Hz, 1H, 3-H$_b$), 3.83 (s, 2H, CH$_2$Br), 3.90–4.13 (m, 4H, 4a-H, 2-H$_2$, 8a-H), 4.29 (m, 1H, 7-H [CH–OH]), 7.15–7.32 (m, 5H$_{ar}$). ^{13}C NMR/^{13}C NMR-APT (75.45 MHz, CDCl$_3$): δ$_C$ 24.41 (1C$_{sec}$, 5-C), 27.22 (1C$_{sec}$, BrCH$_2$C=O), 33.67 (1C$_{sec}$, 8-C), 34.15 (1C$_{sec}$, 3″-C [or 5″-C]), 34.22 (1C$_{sec}$, 5″-C [or 3″-C]), 42.85 (1C$_{tert}$, 4″-C), 42.98 (1C$_{sec}$, 3-C), 50.17 (1C$_{sec}$, 6″-C [or 2″-C]), 52.70 (1C$_{sec}$, 2″-C [or 6″-C]), 57.22 (1C$_{tert}$, 4a-C), 64.85 (1C$_{tert}$, 6-C), 66.11 (1C$_{sec}$, 2-C), 66.83 (1C$_{tert}$, 7-C), 70.13 (1C$_{tert}$, 8a-C), 126.21 (1C$_{tert}$, 4‴-C), 126.95 (2C$_{tert}$, 2‴-C, 6‴-C), 128.50 (2C$_{tert}$, 3‴-C, 5‴-C), 146.50 (1C$_{qu}$, 1‴-C), 167.00 (1C$_{qu}$, BrCH$_2$C=O). MS (ESI) m/z 437.10 {([^{79}Br]M+H)$^+$, 100%}, 439.09 {([^{81}Br]M+H)$^+$, 91%}.

2.2. Radiochemistry

2-[^{18}F]Fluoro-1-[7-hydroxy-6-(4-phenyl-piperidin-1-yl)-octahydro-benzo[1,4]oxazin-4-yl]-ethanone, the [^{18}F]fluoroacetylmorpholino derivative of vesamicol ([^{18}F]FAMV), was obtained by a bromide/fluoride exchange reaction using the N-bromoacetyl derivative (BrAMV) as a precursor compound (Fig. 2).

[^{18}F]Fluoride was produced with a General Electric PETtrace cyclotron. The radiosynthesis of [^{18}F]FAMV was automated using a computer-controlled chemistry module

(TRACERlab FX$_{F-N}$, Nuclear Interface/GE Medical Systems) including preparative high-performance liquid chromatography (HPLC) for purification. The hardware and the controlling system of the module were modified to meet the requirements of the radiosynthesis procedure.

[^{18}F]Fluoride was transformed to a dried [K⊂2.2.2.]$^{+}$/^{18}F^{-} complex. A solution of 3 mg of the BrAMV in dimethylformamide (DMF) was added, and the n.c.a. (no carrier added) nucleophilic substitution of bromine by fluorine was performed at 145–155°C within 15 min.

A C18 Sep-Pak plus cartridge (Waters, Milford, MA, USA) was used to recover most of the radioactivity from the diluted reaction medium as well as to allow passage and separation of [^{18}F]fluoride and hydrophilic side products. [^{18}F]FAMV was eluted from the cartridge by acetonitrile (MeCN). The eluate was diluted with water and subjected to chromatography on a RP 18 column [Kromasil 250×4.6 mm, particle size 10 μm] with a flow rate of 1.25 ml/min. The mobile phase consisted of 50% MeCN and 20 mM ammonium acetate. The [^{18}F]FAMV fractions were collected, diluted with water and concentrated by solid phase extraction (C18 Sep-Pak plus cartridge). [^{18}F]FAMV was eluted with 1.5 ml of ethanol.

Radiochemical and chemical purity of the final product were controlled by analytical HPLC (Nucleosil, 250×ID 4 mm, particle size 5 μm, mobile phase, as described above). The content of solvent residues in the product other than ethanol was determined by gas chromatography.

2.3. Competitive binding assays

The affinity of FAMV to VAChT binding sites, expressed by the K_i value, was determined in equilibrium binding assays via calculation of the concentration of FAMV which was necessary to inhibit the VAChT binding of (−)-[^{3}H] vesamicol by 50% (IC_{50} value) [38].

For comparison, we used: (−)vesamicol hydrochloride (BIOTREND Chemikalien, Cologne, Germany), the *N*-unsubstituted morpholino derivative of vesamicol (Table 2, C), the fluoropropyl-substituted morpholino derivative of vesamicol (Table 2, B) and the σ$_{1/2}$ receptor ligand 1,3-di(2-tolyl)-guanidine (DTG) (BIOTREND Chemikalien), respectively.

PC12 cells stably transfected with a rat VAChT cDNA [9,39] were used as binding target. Assays were performed in 50 mM Tris/HCl buffer, pH 7.4, containing 120 mM NaCl, 5 mM KCl, 2 mM CaCl$_2$ and 1 mM MgCl$_2$ (assay buffer).

For the standard equilibrium assay, 2×10^6 PC12 cells together with 3 pmol (−)-[^{3}H]vesamicol ([^{3}H]2-(4-phenyl-piperidinyl cyclohexanol, specific radioactivity 1258 GBq/mmol, PerkinElmer Life Sciences, Boston, MA, USA) and the relevant compound (in concentrations between 10^{-11} mol/l and 10^{-5} mol/l) were incubated in a volume of 1 ml in duplicate for 2 h at 25°C under agitation (200 min^{-1}). Nonspecific binding was determined in the presence of 10 μM (−)vesamicol. After incubation, the bound form was separated from the free radioligand by a rapid vacuum filtration system (cell harvester Brandel Gaithersburg, MD,

USA) through Whatman GF/B glass-fiber filters presoaked in 0.5% polyethylenimine for 3 h. The filters were washed 3 times with 4 ml ice-cold Tris buffer (0.05 mol/l, pH 7.4). The dried filters were slightly shaken in 10 ml Rotiscint eco plus cocktail (Carl Roth, Karlsruhe, Germany) for about 30 min, maintained in the dark for at least 8 h and then the radioactivity measured in a Tri-Carb2900TR Liquid Scintillation Counter (PerkinElmer Life Sciences) with a 70% counting efficiency.

In addition, compounds were also tested for their binding affinity to σ receptors using rat liver tissue. Rat liver was homogenized in 0.25 M saccharose, and P2 pellets were obtained by centrifugation for 12 min at 40.000*g* at 4°C. The pellets were washed in distilled water and the centrifugation was repeated. In a typical equilibrium assay, duplicate samples containing 900±25 μg protein were incubated with 3 nmol/L of the σ$_{1/2}$ ligand [^{3}H]DTG (specific radioactivity 1110 GBq/mmol, PerkinElmer Life Sciences, Boston, MA, USA) and the relevant test compound (10^{-11} mol/L... 10^{-5} mol/L) in a final volume of 1 ml assay buffer at 25°C under agitation (200 min^{-1}) for 2 h. Nonspecific binding was determined in the presence of 10 μM (−)vesamicol and DTG, respectively. The bound fraction of the radioligand was separated and counted for radioactivity as described above for PC12 cells.

IC_{50} values of FAMV binding were calculated from competitive binding curves by a nonlinear curve fitting, using Graphpad Prism, version 3 (GraphPad Software, San Diego, CA, USA). Specific binding of the radioligand was defined as total binding minus nonspecific binding. The apparent inhibition constant (K_i) was derived from IC_{50} values according to the Cheng-Prusoff equation: $K_i = IC_{50}/(1 + C/K_d)$ [38] where C is the concentration of the radioligand and K_d is the dissociation constant of the radioligand. The K_d value of (−)-[^{3}H]vesamicol for PC12 cells was recently determined (3.74±0.2 nM) [9]. The K_d-value of [^{3}H]DTG for rat liver was reported as 17.9 nM [40].

Each experimentally determined K_i value was the result of at least 5 separate tests performed in duplicates.

2.4. Determination of the lipophilicity of [^{18}F]FAMV

To analyze the lipophilicity of [^{18}F]FAMV, the octanol/water distribution coefficient logD was calculated. Two different approaches were employed. When using the shake-flask method, 50 kBq of [^{18}F]FAMV were added to a conical bottom screw-capped tube containing 1 ml HPLC grade 1-octanol (>99.9% pure, Sigma Chemical, St Louis, MO, USA) saturated with water and 1 ml of veronal acetate buffer pH 7.0. The vial was shaken for 1 h, the mixture centrifuged for 10 min at 6000*g,* and the two liquid phases were separated and placed into counting tubes. The ^{18}F radioactivity was measured in a gamma counter Wizard 1470 (PerkinElmer, Shelton, CT, USA). The logarithm of the radioactivity ratio (D) between the octanol and the aqueous phase was calculated. The values obtained were compared with the estimated logD$_{pH7.0}$ values based on calculations

applying ACD labs/logD calculator (version 4.56, 2000, Advanced Chemistry Development, Toronto, Canada).

2.5. Determination of the plasma protein binding of [^{18}F]FAMV

Plasma protein binding of [^{18}F]FAMV was determined in rat and human plasma samples, which were incubated with [^{18}F]FAMV (20 kBq/ml) at 37°C for 30 min. One milliliter of the labeled plasma was applied on a centrifugal filter device Centrifree containing an YMT30 (cutoff 30,000 MW) membrane (Millipore, Bedford, MA, USA) and equilibrated at 37°C for 10 min. Subsequently, ultrafiltration was performed by centrifugation at 2000g in a 30° fixed-angle rotor (Biofuge primo R, Heraeus, Germany) at 37°C for 6 min. ^{18}F radioactivity was determined in aliquots (100 μl each) of the ultrafiltrate (c_{free}) and of untreated plasma (c_{total}) using a gamma counter 1470 Wizard. Each determination was performed in quadruplicates. The fraction of [^{18}F]FAMV bound to plasma proteins was given as $p = 1 - \frac{c_{free}}{c_{total}}$.

2.6. Determination of the in vitro stability of [^{18}F]FAMV

Human blood samples (5 ml each) were incubated with 0.25 MBq [^{18}F]FAMV at 37°C for 5, 10, 15, 30, 60 and 120 min, respectively. After centrifugation for 5 min at 2000g, plasma proteins were precipitated by addition of 1 ml methanol to 0.5 ml of plasma. The mixture was vigorously vortexed for 2 min and centrifuged for 10 min at 10,000g. The supernatant was subjected to HPLC analysis, as described below, for the determination of radiolabeled metabolites.

2.7. Biodistribution studies

Animal experiments were carried out according to the German Law for the Protection of Animals. For biodistribution studies, 30 female Sprague–Dawley rats (220±15 g) were injected with 5±1.5 MBq [^{18}F]FAMV into their tail veins. The rats were killed under ether anesthesia by decapitation after survival times of 5, 15, 30, 60, 120 and 180 min, respectively. The brain, kidneys, lung, liver and samples of blood, bowel and bone were dissected, weighed and counted for their radioactivity content in a well counter. The results were corrected for radioactive decay and expressed in terms of percent ID per gram of tissue (% ID/g). For each survival time, the data of 5 animals were averaged and expressed as mean±standard deviation.

2.8. Ex vivo rat brain autoradiography

For ex vivo brain autoradiography female Sprague Dawley rats (220±15 g) were injected with 40±5 MBq [^{18}F]FAMV into their tail veins. In selected experiments, rats received an iv injection of 1 μmol/kg of (−)vesamicol hydrochloride at 5 min before radiotracer injection. One hour after radiotracer injection the rats were decapitated, their brains immediately removed, embedded in Tissue-Tek (Sakura Finetechnical, Tokyo, Japan) and frozen using the deep-freeze function of

the cryostat Cryo-Star HM 560 M (MICROM International, Walldorf, Germany). Brains were cut in 20-μm-thick coronal sections, which were placed on gelatin-coated slides. The sections were collected at 200-μm intervals throughout the brain and exposed to FUJIFILM BAS-Imaging plates SR 2025 for 8 h. After exposure, the photostimulated luminescence (PSL) of the imaging plates was measured using a FUJI Bio-Imaging Analyzer BAS 5000. Regions of interest (ROIs) were drawn in the cortex, the striatum, the hippocampus, and the thalamus. The radioactivity in the various ROIs was calculated from the PSL values using radioactivity standards and compared to that in the cerebellum.

2.9. Analysis of metabolites

The metabolism of [^{18}F]FAMV was analyzed in rat blood and brain samples at 5, 30, 60 and 120 min after injection of 50 MBq of the radioligand. Blood samples were centrifuged at 4000g for 6 min at 4°C. To precipitate the plasma proteins, 1 ml methanol was added to 0.5 ml of plasma, vigorously vortexed for 2 min and centrifuged at 10,000g for 10 min. The extraction efficiency of radioactivity was 85%.

Brains were dissected and homogenized using an ULTRA-TURRAX T25 (Janke & Kunkel, Staufen, Germany) in 5 ml of a mixture of ice-cold MeOH, water and triethylamine [70, 30, 0.1 (v/v/v)] for 4×1 min. The mixture was vortexed for 2 min and centrifuged at 10,000g for 10 min. On the average, 60% of the radioactivity could be extracted.

One half of the extract was subjected to chromatography by reversed-phase HPLC (Nucleosil, RP18, 305x7 mm, particle size 5 μm), using a 2-ml injection loop. For separation of [^{18}F]FAMV from metabolites, isocratic conditions (16 min) consisting of a mobile phase of 70, 30 and 0.1 parts (v/v) of methanol, water and triethylamine were used, followed by an acetonitrile gradient up to 100%. During the HPLC separation, the radioactivity of the eluate was measured by the Gabi detector (raytest Isotopenmessgeräte, Straubenhardt, Germany) containing a 3-in. NaI crystal and a detection loop of 1 ml (50 cm of a 1/16-in. capillary). The chromatograms were analyzed using the Chromelion Software (Dionex, Idstein, Germany).

3. Results

3.1. Chemistry and radiochemistry

The yields and analytical data related to the newly developed seven-step synthesis of the parent secondary amine 6-(4-phenyl-piperidin-1-yl)-octahydro-benzo[1,4]oxazin-7-ol. (Fig. 2, **5**), as well as the acylation of the reference substance (FAMV), and of the precursor compound BrAMV for ^{18}F-radiolabelling are described in the materials and methods (Fig. 2). [^{18}F]FAMV was produced (n=37) within 1.6±0.15 h with an radiochemical yield (RCY) of 27±4%. The radiochemical purity of the product was 99±0.8%. The specific activity was between 35 and 125 GBq/μmol. It was observed that most of the precursor

BrAMV was thermically degraded after 15 min at 155°C, whereas [18F]FAMV was stable and remained intact. Hence, [18F]FAMV can be purified effectively by HPLC with a purity≥99%. The content of solvent residues other than ethanol in the final product was <70 µg/ml.

3.2. Lipophilicity of [18F]FAMV

At physiological pH of 7.0, the experimentally determined logD value for FAMV was 1.88±0.3 (n=3). $LogD_{pH\ 7.0}$ values of FAMV, calculated using a computer program (Table 1, $logD_{pH\ 7}$=1.44), also indicate that FAMV is a compound of moderate lipophilicity. Apparently, the annelation of the morpholino structure to the cyclohexanol moiety caused an increase in polarity compared to the analogous compound annelated with a piperidino structure ($logD_{pH\ 7.0}$=2.82).

3.3. Binding assays

The binding affinities of FAMV to VAChT sites and to σ receptor sites were determined in vitro with K_i values of 39.9±5.9 and >1500 nM, respectively (Table 2, compound A). Moreover, the selectivity factor [defined as $K_{i(\sigma\ receptor-binding)}$/$K_{i\ (VAChT\ binding)}$] was >38. For comparison, the enantiomerically pure (−)vesamicol showed a higher affinity to

Table 1

Lipophilicity data: $LogD_{pH\ 7.0}$ values of FAMV determined experimentally ($logD_{pH\ 7.0\ (exp.)}$) and calculated with a computer program (ACDLabs) in comparison to the $logD_{pH\ 7.0\ (calc.)}$ values obtained for the decahydroquinoline analogon of FAMV, vesamicol and benzovesamicol

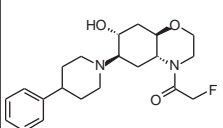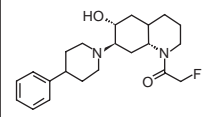| Chemical structure		$LogD_{pH\ 7.0}$ (exp.)	$LogD_{pH\ 7.0}$ (calc.)
	FAMV	1.88±0.3	1.44±0.09
	Decahydroquinoline analogon of FAMV		2.82±0.1
	Vesamicol		1.48±0.09
	Benzovesamicol		2.78±0.09

VAChT (K_i=11.3±1.6 nM) than FAMV but also demonstrated a high affinity to σ receptors (K_i=108.9±24 nM), which resulted in a rather low selectivity factor of 9.6. In comparison to vesamicol, the binding affinity to sigma receptors of the octahydro[1,4]benzoxazines was significantly lower. This is based on the comparatively high K_i values determined for the unsubstituted octahydro[1,4] benzoxazine (Table 2, compound C, K_i>14 µM) as well as for the N-substituted derivatives (Table 2, compound B, K_i>2.5 µM and compound A, K_i>1.5 µM). However, some loss of VAChT binding affinity was also observed when the octahydro[1,4]benzoxazine remained unsubstituted at the secondary amine nitrogen (Table 2, compound C) (K_i=379±51 nM). VAChT binding affinity of compound C was enhanced by substituents such as the aliphatic groups 2-F-acetyl and 3-F-propyl. The fluoroacetylated derivative demonstrated a higher affinity to VAChT binding sites than the fluoropropylated derivative (K_i=39.9±5.9 versus K_i=72.3±10.2 nM). Therefore, the former compound was chosen for radiolabeling (see above).

3.4. Plasma protein binding, brain uptake, and biodistribution of [18F]FAMV

The plasma protein binding of [18F]FAMV was determined as 49±2%. This radiotracer entered the rat brain rather quickly. At 5 min after injection, a brain uptake of 0.12±0.02% ID/g was measured, which subsequently decreased continuously. The cerebellum, known to contain only few cholinergic fibres [41], was used as a reference region to estimate the specific radiotracer uptake. The region-to-cerebellum ratios calculated at 1 h after radiotracer injection in striatum, cortical regions, hippocampus and thalamus were calculated as 4.5±0.4, 2±0.3, 1.5±0.2 and 1±0.2, respectively (Fig. 3). In blood, bone and muscle, a rather low uptake of [18F]FAMV was observed (0.1–0.2% ID/g; Fig. 4). In the lung, the kidney, the liver and the intestine uptake rates of 1.2, 2.6, 2.1 and 2.2% ID/g were measured at 5 min after injection. During the first 15 min of testing, the rate of the uptake in the lung and the kidneys decreased rapidly. Thereafter, a slow and continuous decrease was observed. On the contrary, in the liver and in the intestine, the radiotracer uptake increased during the first 30 min after injection and decreased continuously thereafter.

3.5. Ex vivo autoradiography

Typical autoradiograms of coronal brain slices 1 h after injection of [18F]FAMV show a distinct radiotracer accumulation in the striatum, cortex, olfactory tubercle and in the medial nuclei (Fig. 5). Notably, the highest radiotracer uptake was found in the lateral brain ventricles. The uptake was observed 5 min after injection and increased with time reaching a ventricle-to-cerebellum ratio of 6.0 after 2 h. In addition, the highest uptake was observed in the striatum and in the olfactory tubercle, followed by that in cortical regions. Premedication of rats with 1 µg/kg (−)vesamicol completely
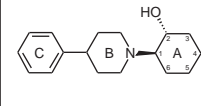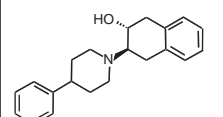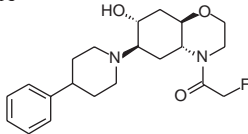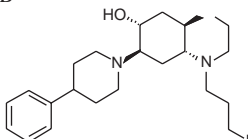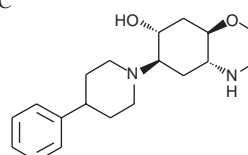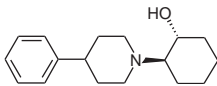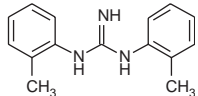
Table 2
Binding affinities of various vesamicol derivatives and DTG to (−)-[3H]vesamicol-labeled VAChT and to [3H]DTG-labelled $\sigma_{1/2}$ receptors

			Affinity to VAChT (K_i, nM)	Affinity to sigma$_{1/2}$ receptors (K_i, nM)	Selectivity factor
2-Fluoro-1-[7-hydroxy-6-(4-phenyl-piperidin-1-yl)-octahydro-benzo[1,4]oxazin-4-yl]-ethanone (FAMV)	A		39.9±5.9	>1500	>37.6
3-Fluoro-1-[7-hydroxy-6-(4-phenyl-piperidin-1-yl)-octahydro-benzo[1,4]oxazin-4-yl]-propanone	B		72.3±10.2	>2500	>34.5
7-hydroxy-6-(4-phenyl-piperidin-1-yl)-octahydro-benzo[1,4]oxazin	C		379.5±51	>14000	>36.8
(-)2-(4-phenylpiperidinyl cyclohexanol ((-)Vesamicol)			1.3±1.6	108.9±24	9.6
1.3-(di-o-tolyl)-guanidine (DTG)			>2200	44.9±6.3	<0.02

K_i values (mean±S.D., $n \geq 6$) were derived from IC_{50} values according to the equation: $K_i = IC_{50}/(1 + C/K_d)$, where C is the concentration of the radioligand and K_d is the dissociation constant of the corresponding radioligand [(−)-[3H]vesamicol binding to VAChT on PC12 cells, K_d=3,7 nM [33]); ([3H]DTG binding to $\sigma_{1/2}$ receptors on rat liver, K_d=17.9 nM [18]).

inhibited the specific binding of [18F]FAMV, resulting in a homogeneous radiotracer distribution (Fig. 5).

3.6. Metabolism of [18F]FAMV in the blood and the brain

A typical time-course of the fraction of unchanged [18F]FAMV in the rat plasma is shown in Fig. 6 (left side triangles). We observed a rapid decrease from 85% at 5 min to 10% at 2 h after injection. In parallel, the amounts of a major and a minor metabolite increased. Also, radioactive metabolites of [18F]FAMV accumulated in brain tissue (Fig. 6, right side), although to a lesser extent than in the plasma. The fate of [18F]FAMV in the brain revealed the formation of fluoride and the presence of two other metabolites. The main metabolite was eluted by HPLC at a retention time of 5 min and reached a fraction of 60% of total radioactivity extracted from the brain. The second metabolite

did not exceed 10% of the total radioactivity during 2 h. No metabolite appeared at a retention time later than that for [18F]FAMV.

4. Discussion

The aim of this study was to develop a PET radioligand for in vivo imaging of the VAChT protein, which is located in cholinergic neurons and represents a well-characterized protein structure with defined binding sites for acetylcholine and vesamicol [8]. To this end, a new vesamicol derivative, [18F]FAMV, was synthesized, radiolabeled, and evaluated in rats.

The results reveal that the radiotracer offers some potential for in vivo neuroimaging studies but needs to be improved in order to become a suitable radioligand for use
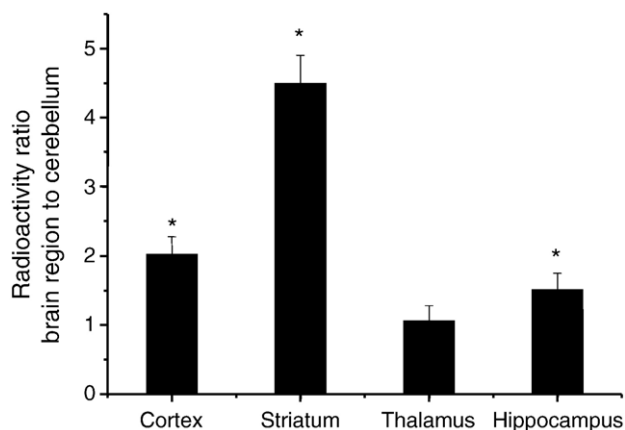
Fig. 3. Accumulation of radioactivity in the rat brain regions containing cholinergic terminals 1 h after injection of 40 MBq [^{18}F]FAMV, measured by ex vivo autoradiography and expressed as ratio between brain region and cerebellum (n=3).

in humans. The following evidence supports our findings and conclusion:

1. [^{18}F]FAMV binds with high affinity to VAChT and shows a good selectivity towards sigma receptors.
2. Ex vivo autoradiography shows the radiotracer accumulation in brain regions with high VAChT densities.
3. Displacement studies reveal specific binding of [^{18}F]FAMV in the brain, except in ventricular areas where high nonspecific accumulation was found.
4. The radiotracer is rapidly metabolized with high accumulation of labeled metabolites in the brain.

The lipophilic amino alcohol 2-(4-phenylpiperidino) cyclohexanol (vesamicol), known for more than 30 years for its anticholinergic potency [42], represents the base chemical structure of all subsequently synthesized compounds for VAChT imaging. So far, no other more promising lead structure than vesamicol has been disclosed. Because of its poor selectivity towards σ$_{1/2}$-receptors [27], efforts are ongoing to synthesize vesamicol-derived analogues possessing an improved specificity in combination with a high binding affinity to VAChT [28,31,33,34,36].

The affinity of vesamicol for VAChT is connected with (i) the typical chair conformation of the molecule, (ii) the nearly coplanar orientated piperidine and cyclohexanol ring structures and (iii) the piperidine nitrogen and the hydroxyl group being in a transposition [16]. Its affinity for VAChT was increased by substituents at the 4-position of the cyclohexanol moiety which are *cis* to the alcohol [37]. The effect of conformational restriction of fragments A and B-C (Fig. 7) was described to increase the selectivity for VAChT over the σ$_{1/2}$-binding sites [27], indicating the free movement of the phenyl and cyclohexanol fragments to be at least partly responsible for the cross reaction to sigma receptors. Considering these results regarding structure–activity relationships from the literature as well as our own negative experience with benzylether derivatives of vesamicol [33],

we developed the bicyclic octahydro-benzo[1,4]oxazin-7-ol structure bearing a 4-phenylpiperidine in position 6. The cyclohexanol moiety contains four stereogenic centers of which those pairs of stereo centers being arranged in opposition are *cis*-configured (Fig. 2, position 6 vs. 8a, and position 7 vs. 4a), whereas both pairs of vicinal stereo centers are *trans*-configured (Fig. 2, position 6 vs. 7 and position 4a vs. 8a). Therefore, it was not surprising that the new compound showed an affinity binding to VAChT in the nanomolar range (K_i=39 nM), which was only slightly different from that of (−)vesamicol (K_i=11 nM). The affinity is expected to further improve after the separation of the respective enantiomeric forms. The structural modifications on the vesamicol molecule performed in this study succeeded in a markedly improved selectivity of FAMV binding to VAChT. The affinity of FAMV to σ receptors was clearly reduced (K_i>1500 nM), which, in comparison to vesamicol, was expressed by a 4-times higher selectivity factor.

The introduction of the oxygen by the morpholino ring structure decreased the lipophilicity of the compound (Table 1, logD$_{pH\ 7.0\ (exp.)}$=1.88, logD$_{pH\ 7.0\ (calc.)}$=1.44) when compared to the decahydroquinoline analogon (Table 1, logD$_{pH7.0\ (calc.)}$=2.82). The aim of this modification was to synthesize less lipophilic fluorinated derivatives of vesamicol with two consequences for their in vivo behavior: (i) a better ratio of specific to unspecific binding and (ii) a faster equilibration between blood pool and nonspecific binding in tissue. However, especially for compounds which enter the brain by perfusion, some degree of lipid solubility is needed for a good passage over the blood–brain barrier to get satisfactory counting statistics [43]. Probably, this level of lipophilicity was not achieved in case of [^{18}F]FAMV because we observed a low brain uptake of [^{18}F]FAMV
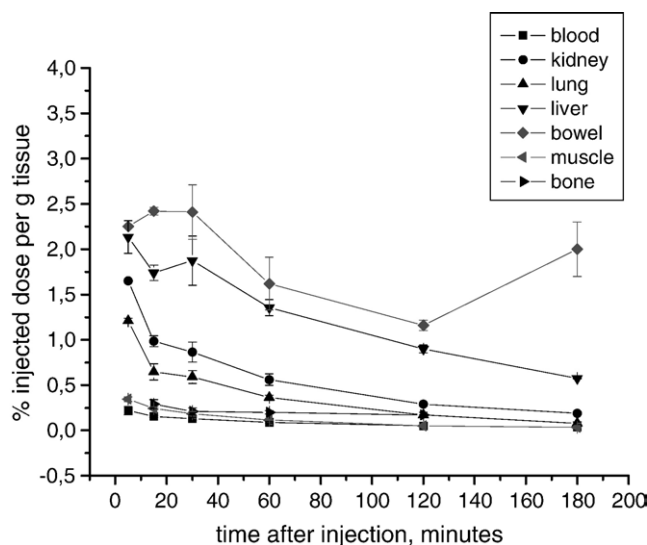

Fig. 4. Distribution of radioactivity in the rat organs, expressed as % injected dose/g, measured at 5, 15, 30, 60, 120 and 180 min after injection of 5±1.2 MBq [^{18}F]FAMV. Each data point represents the mean of data from 6 animals.
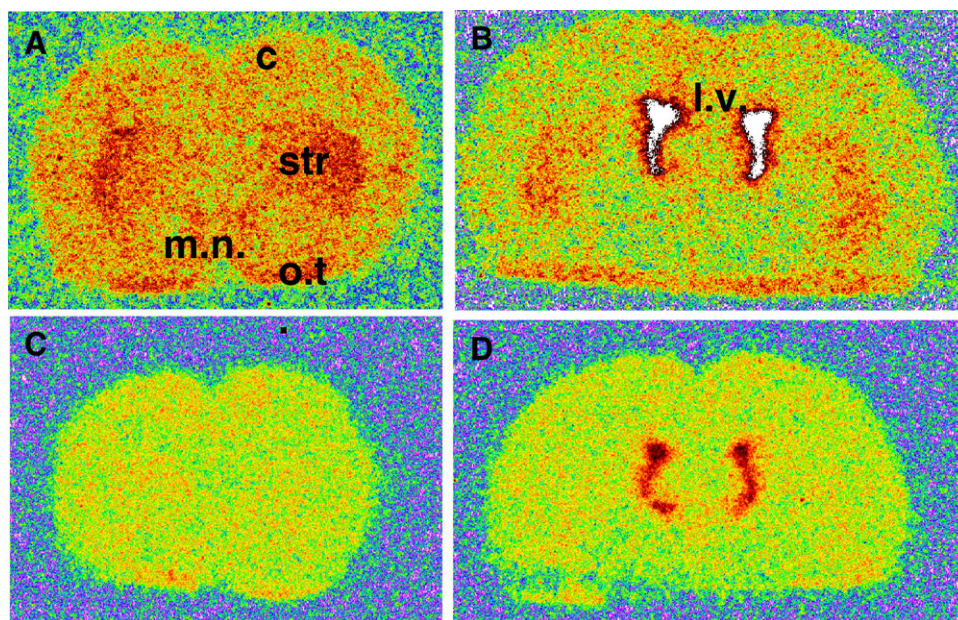
Fig. 5. Ex vivo autoradiography of the rat brain after injection of [^{18}F]FAMV. (A and B) Representative coronal slices of the rat brain 1 h after injection of 40 MBq [^{18}F]FAMV. A high radioactivity concentration was observed in str, followed by o.t., m.n. and c. The highest radioactivity was measured in l.v.. (C and D). Five minutes before injection, of 40 MBq [^{18}F]FAMV the rat received an intravenous injection of 1 μmol/kg of unlabelled (−)vesamicol which was able to displace the specific binding sites in the cortex, the str, o.t. and m.n., but not in the l.v. str, striatum; o.t., olfactory tubercle; m.n., medial nuclei and c, cortex.

(0.04% ID/g) 1 h after injection, which was accompanied by an only moderate brain region-to-cerebellum ratio. The highest ratios at this time were measured in the striatum (4.5) and cortical regions (2.0), and there was no tendency to increase thereafter. The optimal lipophilicity of a new developed derivative of vesamicol seems to be difficult to predict. For example, a low extraction from blood was also described for the strong lipophilic compound [^{18}F]fluor-obenzylamino-benzovesamicol ([^{18}F]FBnABV) [44]. This indicates that the range of appropriate lipophilicity for new

developed vesamicol analogues is rather narrow and/or that lipophilicity is one but not the only factor which regulates brain uptake of these substances.

Nevertheless, brain regions known for their cholinergic innervation, i.e., striatum, cortex and hippocampus, could be visualized using [^{18}F]FAMV by ex vivo autoradiography 1 h after injection. The binding of [^{18}F]FAMV to the vesamicol binding site of VAChT was completely suppressed by a preinjection of unlabeled vesamicol. The biodistribution of [^{18}F]FAMV in rats indicated a favourably low accumulation
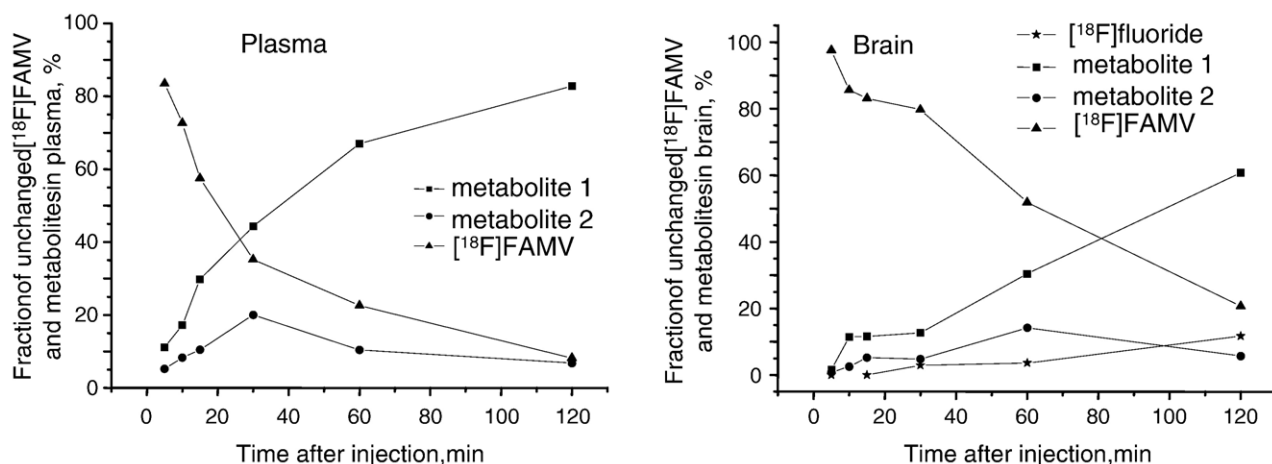
Fig. 6. Typical examples of the reduction of the parent compound and the formation of radioactive metabolites of [^{18}F]FAMV observed in the rat plasma (left) and the rat brain (right) after injection of 40 MBq [^{18}F]FAMV: unchanged [^{18}F]FAMV (▲); main metabolite 1 (■); minor metabolite 2 (●) and fluoride (*). All the compounds were separated by reversed phase HPLC and detected via radioactive decay. Metabolite 1 had a 5 min retention time, and metabolite 2 had a 8–9 min retention time.

Fig. 7. Illustration of the three dimensional structure of vesamicol (left) and the fluoroacetylmorpholino derivative of vesamicol (right).

of radioactivity in the blood, the muscle and the lung tissue. The elimination route of [^{18}F]FAMV mainly directed via the liver and intestine and, to a lesser extent, via the kidneys was similar to that of other fluorinated vesamicol analogues described in the 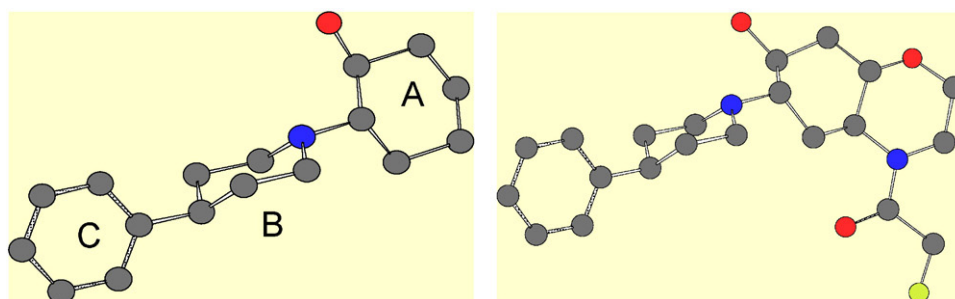literature [44]. It may be assumed that the combination of the rather low brain extraction observed for [^{18}F]FAMV and the plasma protein binding of only 49% did accelerate the elimination of the radioligand from the body.

One of the reasons for the low accumulation in the brain has been found in the marked metabolization of the radioligand, which occurred in the plasma and in the brain tissue. In fact, two metabolites of higher polarity than the parent compound were detected in brain extracts by HPLC analysis. At 30 min after injection, the fraction of unchanged parent compound in the brain was measured at 80% and decreased to 20% after 2 h. The main metabolite of [^{18}F]FAMV is postulated to be [^{18}F]fluoroacetate. Surprisingly [^{18}F]fluoride was detected only in the brain but not in plasma samples, suggesting a brain origin. Recently, it was demonstrated that fluoroacetate is defluorinated by glutathione *S*-transferases [45], which are highly expressed in the brain tissue [46]. The elimination of such radioactive metabolites from the brain tissue may occur via the brain ventricles, where we found accumulation of radioactivity, which was not inhibited by administration of vesamicol (Fig. 5). Another vesamicol derivative ([^{18}F]-*N*-fluoracetamidobenzovesamicol) was also shown to be metabolized in vivo to fluoroacetate [37]. Regarding in vivo stability of new substances, we therefore suggest that the acetate group seems not be an appropriate carrier of [^{18}F]fluorine. Whether the in vivo properties of [^{18}F]FAMV regarding brain extraction, amount of specific accumulation and metabolisation of the radioligand might be more promising in other animals than rats and perhaps in humans, remains speculative. Our future PET studies with [^{18}F]FAMV in pigs are expected to test this hypothesis.

5. Conclusion

In light of in vitro studies on PC12 cells stably transfected with a rat VAChT cDNA, the newly developed [^{18}F]fluoroacetylmorpholino derivative of vesamicol pre-

sented in this study showed high affinity and specificity in binding to VAChT. However, the low extraction of the tracer from blood and its degradation in brain limits the utility of the new compound for in vivo studies, at least in rats. Compounds with different fluorinated substituents at the morpholino nitrogen are presently being tested with respect to their penetration through the blood brain barrier, their in vivo stability and their kinetic behaviour in vivo.

References

[1] Schliebs R, Arendt T. The significance of the cholinergic system in the brain during aging and in Alzheimer's disease. J Neural Transm 2006;113:1625–44.

[2] Sivaprakasam K. Towards a unifying hypothesis of Alzheimer's disease: cholinergic system linked to plaques, tangles and neuroinflammation. Curr Med Chem 2006;13:2179–88.

[3] Whitehouse PJ, Price DL, Struble RG, Clark AW, Coyle JT, Delon MR. Alzheimer's disease and senile dementia: loss of neurons in the basal forebrain. Science 1982;215:1237–9.

[4] Bowen DM, Smith CB, White P, Goodhardt MJ, Spillane JA, Flack RH, et al. Chemical pathology of organic dementias. I. Validity of biochemical measurements on human post-mortem brain specimens. Brain 1977;100:397–426.

[5] Etienne P, Robitaille Y, Wood P, Gauthier S, Nair NP, Quirion R. Nucleus basalis neuronal loss, neuritic plaques and choline acetyltransferase activity in advanced Alzheimer's disease. Neuroscience 1986;19:1279–91.

[6] McGeer PL. The 12th J. A. F. Stevenson memorial lecture. Aging, Alzheimer's disease, and the cholinergic system. Can J Physiol Pharmacol 1984;62:741–54.

[7] Eiden LE. The cholinergic gene locus. J Neurochem 1998;70: 2227–40.

[8] Erickson JD, Varoqui H, Schäfer MKH, Modi W, Diebler MF, Weihe E, et al. Functional identification of a vesicular acetylcholine transporter and its expression from a "cholinergic" gene locus. J Biol Chem 1994;269:21929–32.

[9] Roghani A, Carroll PT. Analysis of uptake and release of newly synthesized acetylcholine in PC12 cells overexpressing the rat vesicular acetylcholine transporter (VAChT). Brain Res Mol Brain Res 2002;100:21–30.

[10] Mallet J, Houhou L, Pajak F, Oda Y, Cervini R, Bejanin S, et al. The cholinergic locus: ChAT and VAChT genes. J Physiol Paris 1998;92: 145–7.

[11] Sihver W, Gillberg PG, Svensson AL, Nordberg A. Autoradiographic comparison of [3H](−)nicotine, [3H]cytisine and [3H]epibatidine binding in relation to vesicular acetylcholine transport sites in the temporal cortex in Alzheimer's disease. Neuroscience 1999;94: 685–96.

[12] Ikeda E, Shiba K, Mori H, Ichikawa A, Sumiya H, Kuji I, et al. Reduction of vesicular acetylcholine transporter in beta-amyloid protein-infused rats with memory impairment. Nucl Med Commun 2000;21:933–7.

[13] Altar CA, Marien MR. [³H]Vesamicol binding in brain: autoradiographic distribution, pharmacology, and effects of cholinergic lesions. Synapse 1988;2:486–93.

[14] Marien MR, Parsons SM, Altar CA. Quantitative autoradiography of brain binding sites fore the vesicular acetylcholine transport blocker 2-(4-phenylpiperidino)cyclohexanol (AH5183). Proc Natl Acad Sci U S A 1987;84:876–80.

[15] Parsons SM, Bahr BA, Rogers GA, Clarkson ED, Noremberg K, Hicks BW. Acetylcholine transporter — vesamicol receptor pharmacology and structure. Prog Brain Res 1993;98:175–81.

[16] Rogers GA, Parsons SM, Anderson DC, Nilsson LM, Bahr BA, Kornreich WD, et al. Synthesis, in vitro acetylcholine-storage-blocking activities, and biological properties of derivatives and analogues of *trans*-2-(4-phenylpiperidino)cyclohexanol (Vesamicol). J Med Chem 1989;32:1217–30.

[17] Browne SE, Lin L, Mattsson A, Georgievska B, Isacson O. Selective antibody-induced cholinergic cell and synapse loss produce sustained hippocampal and cortical hypometabolism with correlated cognitive deficits. Exp Neurol 2001;170:36–47.

[18] Sorger D, Schliebs R, Kampfer I, Rossner S, Heinicke J, Dannenberg C, et al. In vivo [125I]-iodobenzovesamicol binding reflects cortical cholinergic deficiency induced by specific immunolesion of rat basal forebrain cholinergic system. Nucl Med Biol 2000;27:23–31.

[19] Quinlivan M, Chalon S, Vergote J, Henderson J, Katsifis A, Kassiou M, et al. Decreased vesicular acetylcholine transporter and alpha(4) beta(2) nicotinic receptor density in the rat brain following 192 IgG-saporin immunolesioning. Neurosci Lett 2007;415:97–101.

[20] Kish SJ, Distefano LM, Dozic S, Robitaille Y, Rajput A, Deck JHN, et al. [³H]Vesamicol binding in human brain cholinergic deficiency disorders. Neurosci Lett 1990;117:347–52.

[21] Ruberg M, Mayo W, Brice A, Duyckaerts C, Hauw JJ, Simon H, et al. Choline acetyltransferase activity and [³H]Vesamicol binding in the temporal cortex of patients with Alzheimer's disease, Parkinson's disease, and rats with basal forebrain lesions. Neuroscience 1990;35: 327–33.

[22] Efange SMN, Garland EM, Staley JK, Khare AB, Mash DC. Vesicular acetylcholine transporter density and Alzheimer's disease. Neurobiol Aging 1997;18:407–13.

[23] Kuhl DE, Koeppe RA, Fessler JA, Minoshima S, Ackermann RJ, Carey JE, et al. In vivo mapping of cholinergic neurons in the human brain using SPECT and IBVM. J Nucl Med 1993;35:405–10.

[24] Kuhl DE, Minoshima S, Fessler JA, Frey KA, Foster NL, Ficaro EP, et al. In vivo mapping of cholinergic terminals in normal aging. Alzheimer's disease and Parkinson's disease. Ann Neurol 1996;40: 399–410.

[25] Cohen RM. The application of positron-emitting molecular imaging tracers in Alzheimer's disease. Mol Imaging Biol 2007;9:204–16.

[26] Custers FG, Leysen JE, Stoof JC, Herscheid JD. Vesamicol and some of its derivatives: questionable ligands for selectively labelling acetylcholine transporters in rat brain. Eur J Pharmacol 1997;338:177–83.

[27] Efange SM, Mach RH, Smith CR, Khare AB, Foulon C, Akella SK, et al. Vesamicol analogues as sigma ligands. Molecular determinants of selectivity at the vesamicol receptor. Biochem Pharmacol 1995;49: 791–7.

[28] Bando K, Naganuma T, Taguchi K, Ginoza Y, Tanaka Y, Koike K, et al. Piperazine analog of vesamicol: in vitro and in vivo characterization for vesicular acetylcholine transporter. Synapse 2000;38:27–37.

[29] Bando K, Taguchi K, Ginoza Y, Naganuma T, Tanaka Y, Koike K, et al. Synthesis and evaluation of radiolabeled piperazine derivatives of vesamicol as SPECT agents for cholinergic neurons. Nucl Med Biol 2001;28:251–60.

[30] Efange SM, von Hohenberg K, Khare AB, Tu Z, Mach RH, Parsons SM. Synthesis and biological characterization of stable and radio-iodinated (+/−)-*trans*-2-hydroxy-3-P[4-(3-iodophenyl)piperidyl]-1,2,3,4-tetrahydronaphthalene (3'-IBVM). Nucl Med Biol 2000;27: 749–55.

[31] Scheunemann M, Sorger D, Wenzel B, Heinitz K, Schliebs R, Klingner M, et al. Synthesis of novel 4- and 5-substituted benzyl ether derivatives of vesamicol and in vitro evaluation of their binding properties to the vesicular acetylcholine transporter site. Bioorg Med Chem 2004;12:1459–65.

[32] Shiba K, Ogawa K, Ishiwata K, Yajima K, Mori H. Synthesis and binding affinities of methylvesamicol analogs for the acetylcholine transporter and sigma receptor. Bioorg Med Chem 2006;14:2620–6.

[33] Wenzel B, Sorger D, Heinitz K, Scheunemann M, Schliebs R, Steinbach J, et al. Structural changes of benzylether derivatives of vesamicol and their influence on the binding selectivity to the vesicular acetylcholine transporter. Eur J Med Chem 2005;40: 1197–205.

[34] Zea-Ponce Y, Mavel S, Assaad T, Kruse SE, Parsons SM, Emond P, et al. Synthesis and in vitro evaluation of new benzovesamicol analogues as potential imaging probes for the vesicular acetylcholine transporter. Bioorg Med Chem 2005;13:745–53.

[35] Scheunemann M, Sorger D, Kouznetsova E, Sabri O, Schliebs R, Wenzel B, et al. Sequential ring-opening of *trans*-1,4-cyclohaxadiene dioxide for an expedient modular approach to 6,7-disubstituted (±) hexahydro-benzo [1,4]oxazin-3-ones. Tetrahedron Lett 2007;48: 5497–501.

[36] Efange SM, Khare AB, Mach RH, Parsons SM. Hydroxylated decahydroquinolines as ligands for the vesicular acetylcholine transporter: synthesis and biological evaluation. J Med Chem 1999;42: 2862–9.

[37] Rogers GA, Stone-Elander S, Ingvar M, Eriksson L, Parsons SM, Widen L. ¹⁸F-labelled vesamicol derivatives: Syntheses and preliminary in vivo small animal Positron Emission Tomography evaluation. Nucl Med Biol 1994;21:219–30.

[38] Cheng YC, Prusoff WH. Relationship between the inhibition constant (K_i) and the concentration of inhibitor which causes 50% inhibition (IC50) of an enzymatic reaction. Biochem Pharmacol 1973;22: 3099–108.

[39] Roghani A, Feldman J, Kohan SA, Shirzadi A, Gundersen CB, Brecha N, et al. Molecular cloning of a putative vesicular transporter for acetylcholine. Proc Natl Acad Sci U S A 1994;91:10620–4.

[40] Huang Y, Hammond PS, Wu L, Mach RH. Synthesis and structure-activity relationships of N-(1-benzylpiperidin-4-yl)arylacetamide analogues as potent sigma1 receptor ligands. J Med Chem 2001;44: 4404–15.

[41] Arvidsson U, Riedl M, Elde R, Meister B. Vesicular acetylcholine transporter (VAChT) protein: a novel and unique marker for cholinergic neurons in the central and peripheral nervous systems. J Comp Neurol 1997;378:454–67.

[42] Marshall IG. Studies on the blocking action of 2-(4-phenyl piperidino) cyclohexanol (AH5183). Br J Pharmacol 1970;38: 503–16.

[43] Halldin C, Gulyas B, Langer O, Farde L. Brain radioligands — state of the art and new trends. Q J Nucl Med 2001;45:139–52.

[44] Mulholland GK, Wieland DM, Kilbourn MR, Frey KA, Sherman PS, Carey JE, et al. [¹⁸F]fluoroethoxy-benzovesamicol, a PET radiotracer for the vesicular acetylcholine transporter and cholinergic synapses. Synapse 1998;30:263–74.

[45] Tu LQ, Wright PF, Rix CJ, Ahokas JT. Is fluoroacetate-specific defluorinase a glutathione S-transferase? Comp Biochem Physiol C Toxicol Pharmacol 2006;143:59–66.

[46] Johnson JA, el Barbary A, Kornguth SE, Brugge JF, Siegel FL. Glutathione S-transferase isoenzymes in rat brain neurons and glia. J Neurosci 1993;13:2013–23.